NewA, *in press, 27.07.99*

Constraints on Stellar-Dynamical Models of the Orion Nebula Cluster

Pavel Kroupa

MS42, Harvard-Smithsonian Centre for Astrophysics, 60 Garden Street, Cambridge, MA 02138, USA
e-mail: pkroupa@cfa.harvard.edu
(On leave from the Institut für Theoretische Astrophysik, Universität Heidelberg)

Summary

The results obtained by Kroupa, Petr & McCaughrean (1999) for specific models of young compact binary-rich clusters are generalised using dynamical scaling relations, to infer the candidate set of possible birth models leading to the Orion Nebula Cluster (ONC), of which the Trapezium Cluster is the core. It is found that candidate sets of solutions exist which allow the ONC to be in virial equilibrium, expanding or contracting. The range of possible solutions is quite narrow.

These results will serve as guidelines for future, CPU-intensive calculations of the stellar-dynamical and astrophysical evolution of the entire ONC. These, in turn, will be essential to quantify observables that will ultimately discriminate between models, thus allowing us to understand if the ONC is in the process of assembling a rich Galactic cluster, and, if this is the case, how it occurs.

PACS: 98.10.+z; 98.20.-d; 97.80.-d; 97.10.Bt

Subject headings: stars: binaries: general – stars: formation – open clusters and associations: individual (Orion Nebula Cluster, M42)

1. INTRODUCTION

The formation of bound star clusters is a major unsolved problem in observational and theoretical astrophysics. Significant observational (e.g. Lada & Lada 1991; Megeath et al. 1996; Lada, Alves & Lada 1996; Lada, Falgarone & Evans 1997) and theoretical (e.g. Lada, Margulis & Dearborn 1984; Elmegreen & Efremov 1997; Klessen, Burkert & Bate 1998) efforts are being directed at solving this problem. There are serious technical difficulties. For example, on the observational side, the obscuration of a part of the very young stellar and proto-stellar population and significant uncertainties in pre-main sequence evolution (e.g. Wuchterl & Tscharnuter 1999) hamper the understanding of the spatial and age distribution within compact star-forming regions. On the theoretical side, the presently next to impossible handling of three-dimensional self-gravitating magneto-hydrodynamics with feedback from forming stars limits detailed understanding of the onset of star-formation in general, and cluster formation in particular.

This paper forms part of a theoretical approach based on purely stellar-dynamical arguments. These are limited to the phase after the proto-stars and ambient gas decouple dynamically, but allow insights into the evolution of a stellar assemblage after the massive stars rapidly remove the remaining gas. Understanding

this phase of the evolution can provide a lead towards the initial conditions that give rise to bound Galactic clusters.

Stellar-dynamical calculations of binary-rich young compact clusters with Aarseth's NBODY5 code were presented by Kroupa, Petr & McCaughrean (1999, hereinafter KPM), to study the evolution of the binary population and of the cluster bulk properties. The results were applied to a comparison with key observables available for the Trapezium Cluster, and a solution was found in which the Trapezium Cluster, with a stellar mass of $700\,M_\odot$, is expanding rapidly due to the expulsion of about $1000\,M_\odot$ in gas roughly 50 000 yr ago. However, while that work quantifies the evolution of the binary population and of the cluster within a few Myr, the question remains open as to how unique the expanding solution of the Trapezium Cluster is.

In this paper the solution space of all possible models of the ONC is studied by invoking stellar-dynamical scaling relations that capture the gross behaviour of star clusters, and by building on the results obtained by KPM. Section 2 summarises the key observables used to constrain the allowed range of models, and in Section 4 the KPM results are generalised and the candidate solution space is identified. The conclusions follow in Section 5.

2. OBSERVATIONAL CONSTRAINTS

A detailed description of the observational constraints can be found in KPM. Here a brief summary is given. The key observables used to constrain the stellar-dynamical models by KPM are the central stellar number density, the pre-main-sequence age of the stellar population, the velocity dispersion, and the binary proportion.

Based on a high-spatial-resolution direct-imaging near-infrared study, McCaughrean & Stauffer (1994) calculate that 29 systems are within the central spherical volume with a radius of $R = 0.053$ pc. This corresponds to a central number density $\rho_{\rm c}^{\rm (obs)} = 4.65 \times 10^4$ stars/pc^3 (strictly speaking systems/pc^3, but the maximal factor of 2 error is not critical in this analysis). In a near-infrared study covering a field of $\sim 0.65\,{\rm pc} \times 0.65\,{\rm pc}$ centred on the Trapezium Cluster, McCaughrean et al. (1996) count 700 systems.

From the analysis of the HR-Diagram, based on optical photometry and spectroscopy, Prosser et al. (1994), Hillenbrand (1997) and Palla & Stahler (1999) derive a mean age for the whole Orion Nebula Cluster of less than about 1 Myr.

The one-dimensional velocity dispersion within 0.41 pc of the centre of the Trapezium Cluster is derived by Jones & Walker (1988), from their relative proper-motion survey using photographic plates, to be $\sigma^{\rm (obs)} = 2.54 \pm 0.27$ km/s. Because the plate-reduction algorithms eliminate any signature due to rotation and/or expansion or contraction, it is unknown from that work and others (see KPM) if the Trapezium Cluster is expanding or contracting. Frink, Kroupa & Röser (1999) measure the bulk motions in the ONC using new absolute proper motion data, and find some expanding as well as contracting motion. Their result is consistent with the ONC currently expanding in an approximately cylindrical molecular cloud potential (Kroupa & Frink 1999). Following KPM the velocity dispersion obtained from the more precise relative proper motions is used in the present analysis.

High-resolution imaging using a variety of techniques has shown that the binary proportion within about 0.3 pc of the centre of the Trapezium Cluster is significantly below that seen in Taurus–Auriga, but consistent with the Galactic field value (Prosser et al. 1994; Petr 1998; Petr et al. 1998). This may be the

result of disruption through encounters in the cluster (KPM).

The Trapezium Cluster contains virtually no gas (Wilson et al. 1997), and a large part of the ONC population is optically visible (Hillenbrand & Hartmann 1998), so that purely stellar-dynamical calculations can be applied.

There is little evidence for sub-structure in the ONC (Bate, Clarke & McCaughrean 1998).

3. THE KPM STELLAR-DYNAMICAL MODELS

Details are found in KPM. The KPM models contain $N = 1600$ stars (cluster mass $M_{\rm cl} = 700\,M_\odot$), with a Galactic-field IMF with stellar masses in the range $0.08\,M_\odot$ to $30\,M_\odot$. The stars are paired at random to form a primordial binary proportion of unity, $f_{\rm tot} = 1$ with a period distribution as seen in Taurus–Auriga, and $f_{\rm tot} = 0.6$ with a period distribution as in the Galactic field. Here, the total (counting all separations) binary proportion is $f_{\rm tot} = N_{\rm bin}/(N_{\rm bin} + N_{\rm sing})$, where $N_{\rm bin}$ and $N_{\rm sing}$ are the number of binary and single-star systems, respectively. Stellar evolution is not treated, and the dynamical evolution is followed for 5 Myr only.

Six different models are constructed to cover a range of possible cases, each having initially a Plummer density profile with half-mass radius $R_{0.5}$:

- Virial equilibrium models with primordial $f_{\rm tot} = 1$ (model A1) and $f_{\rm tot} = 0.6$ (model A2). These have initially $R_{0.5} = 0.1$ pc, $t_{\rm cross} = 0.06$ Myr (eqn. 2) and $t_{\rm relax} = 0.62$ Myr (eqn. 3).
- Expanding clusters assuming a star formation efficiency $\epsilon = M_{\rm cl}/(M_{\rm cl} + M_{\rm gas}) = 0.42$ and instantaneous loss of a gas mass $M_{\rm gas} = 967\,M_\odot$ at the start of the computation, with binary proportions $f_{\rm tot} = 1$ (model B1) and 0.6 (model B2). These models have $R_{0.5} = 0.1$ pc and an initial velocity dispersion that is $\epsilon^{-1/2}$ larger than the virial equilibrium value without the gas.
- Clusters that collapse with an initial velocity dispersion that is a factor 0.14 times smaller than the virial equilibrium value, with initially $R_{0.5} = 0.4$ pc (model C1) and 0.8 pc (model C2). These have $f_{\rm tot} = 1$.

Three renditions of each model yield averages of the relevant observables.

The choice for N is based on the observed number of systems in the Trapezium Cluster. The initial central density ($\rho_{\rm c,in} = 10^{5.92}$ stars/pc^3) of the virial equilibrium and expanding models is larger than the presently observed value ($\rho_{\rm c}^{\rm (obs)} = 10^{4.67}$ stars/pc^3), because a reduction of the central density with time is anticipated without knowing the detailed evolution in advance, since no such compact and binary-rich clusters had ever been evolved until then. For the collapsing models, the initial possible configuration is unknown, since N-body collapse calculations of an initially centrally concentrated density profile and with a large proportion of realistic binary systems had never been done before. The values $R_{0.5} = 0.4$ and 0.8 pc are thus first tries.

The mean stellar mass is $0.44\,M_\odot$. It is used throughout this paper: $M_{\rm cl} = 0.44 \times N\,M_\odot$.

4. GENERALISATION

Before constraining the solution space using dynamical arguments, a pre-selection can be made immediately, by noting that the lower limit on N is 700 stars, since this many systems have been counted in the Trapezium Cluster (Section 2).

It is known that the binary fraction is high (about 50–60 per cent), so N is likely to be closer to 1200. However, since some loss of stars is expected through dynamical ejection, and in general location at larger radii than the survey limit, $N = 1600$ is deemed more appropriate to be a lower limit. There is thus little room for an initial N below about 1600.

Assuming the Trapezium Cluster is merely the core of the ONC, an upper limit $N = 5600 - 10000$ is obtained for the whole ONC. The lower value is valid if the overall binary proportion is $f_{\rm tot} = 0.6$, since about 3500 systems have been counted within approximately 2.5 pc of the cluster's centre (Hillenbrand & Hartmann 1998). The upper limit is estimated by assuming $f_{\rm tot} = 1$ as a probably more realistic value for most of the ONC, implying that 7000 stars will have been counted, and that 30 per cent of all systems have been lost through expansion beyond the 2.5 pc radius, or have not been seen because they are too deeply embedded or too faint.

4.1. Clusters in virial equilibrium

Without doing additional time-consuming numerical experiments, the evolution of model clusters in virial equilibrium with different N and $R_{0.5}$ can be assessed through simple scaling arguments.

Binary depletion occurs approximately on a crossing time-scale, $t_{\rm cross}$ (fig. 3 in KPM), whereas the velocity dispersion and central density change on a time-scale comparable to the relaxation time, $t_{\rm relax}$ (fig. 2 in KPM). That complete destruction of long-period or soft binaries occurs within a few tens of initial $t_{\rm cross}$ is demonstrated in Fig. 1, in which the evolution of $f_{\rm tot}$ for two very different clusters is compared. Despite very different initial crossing times and different N, $f_{\rm tot}$ decays on a comparable time-scale $\approx$ few $\times\, t_{\rm cross}$. That the decay is not exactly in-phase does not affect the conclusions of this paper.

The three-dimensional velocity dispersion,

$$\sigma = s \left(\frac{G\, M_{\rm cl}}{2\, R_{0.5}} \right)^{\frac{1}{2}}, \tag{1}$$

where $G = 4.49 \times 10^{-3}\,{\rm pc}^3/(M_\odot\,{\rm Myr}^2)$ is the gravitational constant, and s is a structure constant of order unity defined by the details of the density distribution. The one-dimensional velocity dispersion is $\sigma_{\rm 1D} = \sigma/\sqrt{3}$, assuming the velocity distribution is isotropic. For $M_{\rm cl} = 700\,M_\odot$ and $R_{0.5} = 0.1$ pc, $\sigma_{\rm 1D}/s = 2.29$ pc/Myr (1 pc/Myr= 0.982 km/s, but throughout this paper no distinction is made between these two units), and from fig. 2 in KPM, $\sigma_{\rm 1D}(t=0) = 1.95$ km/s, so that $s = 0.85$ throughout this paper.

The typical crossing time,

$$t_{\rm cross} = \frac{2\, R_{0.5}}{\sigma}, \tag{2}$$

whereas the relaxation time in Myr (from Binney & Tremaine 1987),

$$t_{\rm relax} \;=\; \frac{21}{\ln(0.4\,N)} \left(\frac{M_{\rm cl}}{100\,M_\odot} \right)^{1/2} \left(\frac{1\,M_\odot}{\overline{m}} \right) \left(\frac{R_{0.5}}{1\,{\rm pc}} \right)^{3/2} . \tag{3}$$

Thus, it is immediately apparent that increasing N (i.e. $M_{\rm cl}$) will, for the same $R_{0.5}$, *shorten* the time-scale for binary depletion while simultaneously *slowing down* the time-scale for the evolution of the central density and velocity dispersion. This implies that by increasing N, the variation of the central density becomes increasingly negligible over the age of the cluster. This is already evident in fig. 2 in KPM, where the central density decays by a factor of 2.5 only during the first Myr. The central density for a Plummer density distribution is

$$\rho_{\rm c} = \frac{3\,N}{4\,\pi\,\left(0.77\,R_{0.5}\right)^3}, \tag{4}$$

where $R_{\rm pl} = 0.77\,R_{0.5}$ is the Plummer radius.

For illustrative purposes, two sets of initial models are constructed and compared in Fig. 2. One set of models has $\log_{10}(\rho_{\rm c}) = 5.92$ (stars/pc^3), which is the same as in models A. The other set has $\log_{10}(\rho_{\rm c}) = 4.67$ (stars/pc^3), which is the same as the observed central density in the Trapezium Cluster. The first set is clearly not a viable solution set since the initial density remains too high ($t_{\rm relax}$ is too long).

However, there is a set of virial-equilibrium candidate solutions if $10000 \lesssim N \lesssim 16000$ and $0.48 \lesssim R_{0.5} \lesssim 0.61$, for the constraint $\rho_{\rm c} = $constant. These models have a velocity dispersion consistent with the observed value, and $t_{\rm cross} = 2.5 \times 10^5$ yr, which is sufficiently short for significant binary depletion to have occurred in the ONC until now (Fig. 1). Fully self-consistent N-body calculations are needed to verify if a Taurus–Auriga-like binary population can be reduced to the observed level in the Trapezium Cluster. The calculations of KPM suggest that this is likely to be the case.

Relaxing the constant-central density constraint, the full set of candidate solutions is obtained (Fig. 3). As already apparent in Fig. 2, the set of presumed solutions is *very narrow*, with $N \approx 10^4$, $M_{\rm cl} \approx 4.4 \times 10^3\,M_\odot$ and $R_{0.5} \approx 0.45$ pc. It has been known for a long time that the velocity dispersion in the Trapezium Cluster is super-virial, if only the number of detected stars is used to estimate the cluster mass (e.g. Hillenbrand & Hartmann 1998). However, the candidate solutions found here demonstrate that, by taking into account the binary companions, the natural loss of stars from the cluster through its dynamical evolution, and allowing for a small fraction of stars not detected yet, a model of the initial ONC is found that is remarkably close to virial equilibrium.

4.2. Expanding clusters

Model B2 in KPM shows that if the Trapezium Cluster is expanding then it is being observed now at a time when the velocity dispersion and central density have not decayed so much as to make the system appear like an association. Expansion must have begun a few tens of thousands of years ago, and the initial $f_{\rm tot}$ must have been similar to that in the Galactic field, and thus significantly below that in Taurus–Auriga. Model B2 assumes a high star-formation efficiency of $\epsilon = 0.42$, which nevertheless leads to an essentially rapid free expansion of the entire system (Kroupa & Frink 1999). Indeed, Lada, Margulis & Dearborn (1984) demonstrate that, if $\epsilon < 0.5$ and gas is removed instantaneously, then an unbound, expanding association results. The presence of a few O stars in the Trapezium Cluster suggests that the removal of gas occurred on a time-scale comparable to or shorter than a crossing time.

The set of candidate solutions to an expanding Trapezium Cluster, assuming instantaneous gas removal and virial equilibrium of the stellar and gaseous system before gas expulsion, can be constrained by noting that the pre-expansion central density and velocity dispersion must have been larger than the presently observed values, $\rho_{\rm c}(t=0) > \rho_{\rm c}^{\rm (obs)}$ and $\sigma_{\rm 1D}(t=0) > \sigma^{\rm (obs)}$, where $t = 0$ refers to the gas-expulsion time.

The central density cannot be made arbitrarily large, since binary systems with semi-major axes as large as $a = 440$ AU exist in abundance (section 2.3 in KPM). Thus, if each binary system needs a volume with a radius $\gamma\, a$ to form, and the forming systems touch, then the maximum number density would be

$$\rho_{\rm c}^{\rm max} = \frac{3\times 2}{4\,\pi\,(\gamma\, a)^3}, \tag{5}$$

so that $\rho_{\rm c}^{\rm max} = 10^{7.69} - 10^{4.69}$ stars pc^{-3} for $\gamma = 1 - 10$.

In a freely expanding flow that is unhindered by self-gravity, the velocity dispersion measured within a projected volume with a constant radius $2\,R$ decreases with time according to

$$\sigma_{\rm 1D}(t) = \frac{R}{t + R/\sigma_{\rm 1D}(0)}, \tag{6}$$

where $\sigma_{\rm 1D}(0) = \sigma_{\rm 1D}/\sqrt{\epsilon}$ is the velocity dispersion before gas expulsion, and $\sigma_{\rm 1D}$ is, as in Section 4.1, the velocity dispersion of the stellar cluster if it were in virial equilibrium and without gas (eqn. 1). This equation ensures that the initial velocity dispersion, $\sigma_{\rm 1D}(0)$, is arrived at, and essentially measures the typical velocity, R/t, of the stars remaining in the measurement area. The term $R/\sigma_{\rm 1D}(0)$ is the time-lag until stars with typical velocity $\sigma_{\rm 1D}(0)$ leave the area. The velocity-dispersion model-data corrected for the radial bulk flow plotted in the bottom panel of fig. 6 in KPM fit this relation very well with $R = 0.21$ pc. That the flow in the KPM models B is free on scales larger than a few tenths of a pc is also demonstrated in Kroupa & Frink (1999). The time at which $\sigma_{\rm 1D}(t_{\rm exp}) = \sigma^{\rm (obs)} = 2.54 \pm 0.27$ km/s is

$$t_{\rm exp} = R\,(\frac{1}{\sigma^{\rm (obs)}} - \frac{1}{\sigma_{\rm 1D}(0)}). \tag{7}$$

In a free radial expansion flow, the central density in a Plummer density distribution should evolve as

$$\rho_{\rm c}(t) = \frac{3\,N}{4\,\pi\,R_{\rm pl}(t)^3}, \tag{8}$$

because the Plummer radius of the system increases with time as $R_{\rm pl}(t) = 0.77\,R_{0.5} + \sigma(0)\,t$. However, the model data plotted in the upper panel of fig. 6 in KPM show that the real central density, evaluated within a radius $R = 0.053$ pc, decreases much less rapidly. This is due to stellar-dynamical interactions in the binary-rich system leading to a part of the population decoupling from the flow and forming a small bound cluster, as discussed in section 5.2.1 in KPM. Cooling of the flow through some binary destruction appears to be instrumental in forming this decoupled core, as can be inferred by comparing the central densities of models B1 and B2 at $t > 0.2$ Myr in fig. 6 of KPM. This mode of cluster formation will be addressed in more detail in a future contribution. For the present, it has to be accepted that the evolution of $\rho_{\rm c}(t)$ cannot be expressed analytically.

A set of possible initial models is summarised in Fig. 4. Surmised solutions with $N = 1600$ and a star-formation efficiency of 42 per cent have $R_{0.5} < 0.12$ pc, ensuring that the pre-expansion velocity dispersion is larger than the observed value by at least a one-sigma error margin. Such models lead to the velocity dispersion being consistent with the observed value within $t \lesssim 10^5$ yr. For $\epsilon = 0.1$, the candidate solutions have $R_{0.5} < 0.27$ pc, ensuring the pre-expansion central density is larger than the currently observed value. In this case the pre-expansion velocity dispersion is very large, requiring a longer time to pass until the velocity dispersion has decayed to a value consistent with that observed. Nevertheless, $t_{\rm exp} < 10^5$ yr. Candidate solutions with $N = 10^4$ have $R_{0.5} < 0.47$ pc and $t_{\rm exp} \lesssim 10^5$ yr for $\epsilon \leq 0.42$.

The full set of candidate solutions is shown in Fig. 5. For all candidate solutions, $t_{\rm exp} < 1.2 \times 10^5$ yr. The KPM calculations show that $f_{\rm tot}$ does not evolve significantly, so that $f_{\rm tot} \approx 0.6$ is required at the time when expansion ensues.

4.3. Collapsing clusters

An initially homogeneous sphere with radius $R_{\rm in}$ that starts from rest collapses to a singularity under its own gravity within a free-fall time, $t_{\rm col} \approx t_{\rm cross}/\sqrt{2}$ (e.g. Binney & Tremaine 1987). If the initial matter distribution is not smooth, for example when only a finite number of stars is present, local density differences will lead to the growth of the tangential velocity dispersion which limits the radius of the collapse to the minimum value at the bounce (Aarseth, Lin & Papaloizou 1988)

$$R_{\rm b} \approx R_{\rm in}/N^{1/3}. \tag{9}$$

The post-collapse system exhibits a core-halo structure, and an initial asphericity will be retained to some degree by the halo, whereas the core will be approximately spherical (Boily, Clarke & Murray 1999). This may, in principle, be a model of the ONC, which has an approximately spherical core (the Trapezium Cluster) and an elliptical halo (Hillenbrand & Hartmann 1998), provided the ONC is old enough for the collapse to have progressed to the morphology evident today.

The presence of a large number of primordial binary systems complicates the situation dramatically because they have relatively large interaction cross sections, and they constitute an energy sink as well as a highly significant energy source. A cold collapse can be envisioned being arrested when the densities become large enough that the binary systems begin interacting. At this stage cooling through binary disruption will reduce the relative velocities between the systems, slowing down the collapse. Additionally, heating through hardening binaries will also oppose the collapse. Vesperini & Chernoff (1996) address such issues by considering the collapse of an initially homogeneous sphere with a binary proportion $f_{\rm fot} = 0.05$. They find that the primordial binaries do not alter the collapse and violent relaxation. However, their results are not applicable to the present work, since the binary proportion used here is significantly higher, and because the results of Vesperini & Chernoff apply to the case where binary–binary collisions are insignificant. Binary–binary collisions, however, dominate the interactions in the realistic case considered here. Details of the processes await further research.

During a cold collapse starting from an initially spherical and homogeneous configuration with initial (central) density $\rho_{\rm c,in}$, the central density increases to a value at the bounce $\rho_{\rm c,b} \approx N \times \rho_{\rm c,in}$, given the above scaling for the linear dimension of the system. This is not fulfilled in models C1 and C2, since this scaling and eqn. 4 for $\rho_{\rm c,in}$, would imply $\rho_{\rm c,b}^{\rm C1} = 10^{7.3}$ [stars/pc^3] and $\rho_{\rm c,b}^{\rm C2} = 10^{6.5}$ [stars/pc^3], whereas from fig. 10 in KPM values of $10^{5.9}$ and $10^{5.8}$ stars/pc^3, respectively, result in the collapse computations. The central density at bounce is significantly smaller because (i) the models have a small but finite initial velocity dispersion, (ii) the initial density distribution is centrally concentrated leading to a spread of arrival times near the centre which increases $R_{\rm b}$, and (iii) binary systems oppose the collapse.

Similarly, the one-dimensional velocity dispersion of the system at bounce cannot be calculated from a simple scaling law, because at this stage it is unknown how the binding energy of the binary-rich initially centrally concentrated cluster evolves. However, the data in the lower panel of fig. 10 in KPM suggest that, if $\sigma_{\rm vir,in}$ is the one-dimensional velocity dispersion a pre-collapse cluster would have were it in virial equilibrium (eqn. 1), then

$$\sigma_{\rm b} = 1.71 \times \sigma_{\rm vir,in}. \tag{10}$$

For models C1 and C2, the one-dimensional velocity dispersion $\sigma_{\rm vir,in} = 0.97$ km/s and 0.69 km/s (eqn. 1), respectively, so that $\sigma_{\rm b}^{\rm C1} \approx 1.62$ km/s and $\sigma_{\rm b}^{\rm C1} \approx 1.20$ km/s. Useful constraints can be placed on the candidate solution-set of pre-collapse models of the ONC if eqn. 10 is adopted for a comparison with $\sigma^{\rm (obs)}$.

The one-dimensional velocity dispersion at bounce must be *larger* than or equal to the observed value $\sigma_{\rm b} \gtrsim \sigma^{\rm (obs)}$. Also, the initial central density must be smaller than or equal to the presently observed value, $\rho_{\rm c,in} \leq \rho_{\rm c}^{\rm (obs)}$. In addition, the collapse time must be short enough to be consistent with the pre-main sequence age of the Trapezium Cluster, $t_{\rm col} \lesssim 1$ Myr, since the cluster could not have been collapsing stellar-dynamically for a time longer than the age of the stars.

The collapse time $t_{\rm col} \propto t_{\rm cross}$, where $t_{\rm cross}$ is the crossing time of the pre-collapse cluster (eqn. 2). To estimate the constant of proportionality, the data presented in fig. 10 of KPM need to be resorted to again. The result is

$$t_{\rm col} = 0.97 \times t_{\rm cross}. \tag{11}$$

Sequences of initial models are constructed for $N = 1600$ and 10^4, and $\rho_{\rm c,in}$, $t_{\rm col}$ and $\sigma_{\rm b}$ are calculated for each as a function of $R_{0.5}$. The results are presented in Fig. 6. There is no candidate set of solutions for $N = 1600$, because the velocity dispersion at the bounce never reaches the observed value for those cases when the central pre-collapse density is smaller than the observed central density in the Trapezium Cluster. However, there is a candidate solution set for models with $N = 10^4$. Such models have $0.5 < R_{0.5} < 1.2$ pc and should satisfy the observational constraints at some time $\lesssim 1$ Myr during collapse. Detailed N-body calculations are required to verify if this is indeed a viable solution set, and if the central density and velocity dispersion pass through the observational constraints at about the same time.

The full set of candidate solutions is shown in Fig. 7. The results of KPM illustrate that $f_{\rm tot}$ decreases significantly during $1 - 2 \times t_{\rm col}$, but that the binary proportion after virialisation depends on the initial $R_{0.5}$. Thus, it is likely that initial $f_{\rm tot} < 1$ (i.e. a smaller binary proportion than in Taurus–Auriga) will be necessary for presumed solutions with $R_{0.5} > 0.5$ pc, to account for the observed binary proportion in the Trapezium Cluster. Detailed N–body calculations are needed to address this issue.

4.4. Caveats

The models investigated here assume the clusters initially have spherical and smooth Plummer density profiles. Deviations from this will not change the results significantly for the same $\rho_{\rm c}$, $M_{\rm cl}$ and $R_{0.5}$. A complication that will have to be incorporated in future studies of the evolution of the ONC is the tidal field exerted across it from the nearby molecular cloud. Kroupa & Frink (1999) show that the overall shape and velocity field of an expanding young cluster can be affected noticeably in such a case.

5. CONCLUSIONS

Using stellar-dynamical scaling laws together with results from N-body calculations, three general classes of possible stellar-dynamical solutions to initial configurations of the ONC (and of the Trapezium Cluster) are investigated. By doing so, candidate initial models have been found for all three classes. Thus, the ONC may presently be (i) in or close to virial equilibrium, (ii) expanding, or (iii) collapsing or in violent relaxation following a cold collapse. Class (i) only allows a candidate solution in virial equilibrium with $R_{0.5} \approx 0.45$ pc and $N \approx 10^4$. Such a large N is realistic only if the binary proportion in the ONC (rather

than the Trapezium Cluster) is close to unity, and if about 30 per cent of stars are not detected and/or have already been ejected to radii of a few pc or larger.

The first and third classes will undoubtedly lead to a bound Galactic cluster, while the second is likely to, on the basis of the formation of a small bound cluster in the expanding Trapezium-Cluster models of KPM. The present results thus show that the ONC is most probably forming a Galactic cluster. It is unclear though by which of the three paths above this is occurring.

However, only *candidate* initial models have been presented here. Follow-up, CPU-intensive N-body calculations will have to be performed to verify which of these are consistent with the observational constraints. The constraints include the velocity dispersion, mass segregation, and the binary-proportion and density profiles in the ONC.

Acknowledgements

I am thankful to Chris Boily for useful correspondence, and Sverre Aarseth for helpful discussions. I acknowledge support from DFG grant KR1635 and a short-visitor grant from the Smithsonian Institution.

REFERENCES

Aarseth S.J., Lin D.N.C., Papaloizou J.C.B., 1988, ApJ, 324, 288

Bate M.R., Clarke C.J., McCaughrean M.J., 1998, MNRAS, 297, 1163

Binney J., Tremaine S., 1987, Galactic Dynamics, Princeton University Press, Princeton

Boily C.M., Clarke C.J., Murray S.D., 1999, MNRAS, 302, 399

Elmegreen B.G., Efremov Yu.N., 1997, ApJ, 480, 235

Frink S., Kroupa P., Röser S., 1999, MNRAS, submitted

Hillenbrand L.A., 1997, AJ, 113, 1733

Hillenbrand L.A., Hartmann L.W., 1998, ApJ, 492, 540

Jones B.F., Walker M.F., 1988, AJ, 95, 1755

Klessen R.S., Burkert A., Bate M.R., 1998, ApJ, 501, 205

Kroupa P., 1995, MNRAS, 277, 1491

Kroupa P., Frink S., 1999, MNRAS, submitted

Kroupa P., Petr M., McCaughrean M.J. 1999, NewA, in press, astro-ph/9906460 (KPM)

Lada C.J., Lada E.A. 1991, in The Formation and Evolution of Star Clusters, ed. K. Janes, ASP Conf. Ser. vol.13, p3

Lada C.J., Alves J., Lada E.A., 1996 AJ, 111, 1964

Lada E.A., Falgarone E., Evans N.J., 1997, ApJ, 488, 286

Lada C.J., Margulis M., Dearborn D., 1984, ApJ 285, 141

McCaughrean M.J., Stauffer J.R., 1994, AJ, 108, 1382

McCaughrean M.J., Rayner J.T., Zinnecker H., Stauffer J.R., 1996, in Beckwith S.V.W., Staude J., Quetz A., Natta A., eds., Disks and Outflows around Young Stars, Lecture Notes in Physics, 465, Heidelberg, Springer, p.33

Megeath S.T., Herter T., Beichman C., Gautier N., Hester J.J., Rayner J., Shupe D., 1996, A&A, 307, 775

Palla F., Stahler S.W., 1999, ApJ, in press

Petr M.G., 1998, Binary Stars in the Orion Trapezium Cluster: A High angular Resolution Near-Infrared Imaging Study, PhD thesis, University of Heidelberg

Petr M.G., Coudé du Foresto V., Beckwith S.V.W., Richichi A., McCaughrean M.J., 1998, ApJ, 500, 825

Prosser C.F., Stauffer J.R., Hartmann L.W., Soderblom D.R., Jones B.F., Werner M.W., McCaughrean M.J., 1994, ApJ, 421, 517

Vesperini E., Chernoff D.F., 1996, ApJ, 458, 178

Wilson T.L., Filges L., Codella C., Reich W., Reich P., 1997, A&A, 327, 1177

Wuchterl G., Tscharnuter W.M., 1999, A&A, submitted

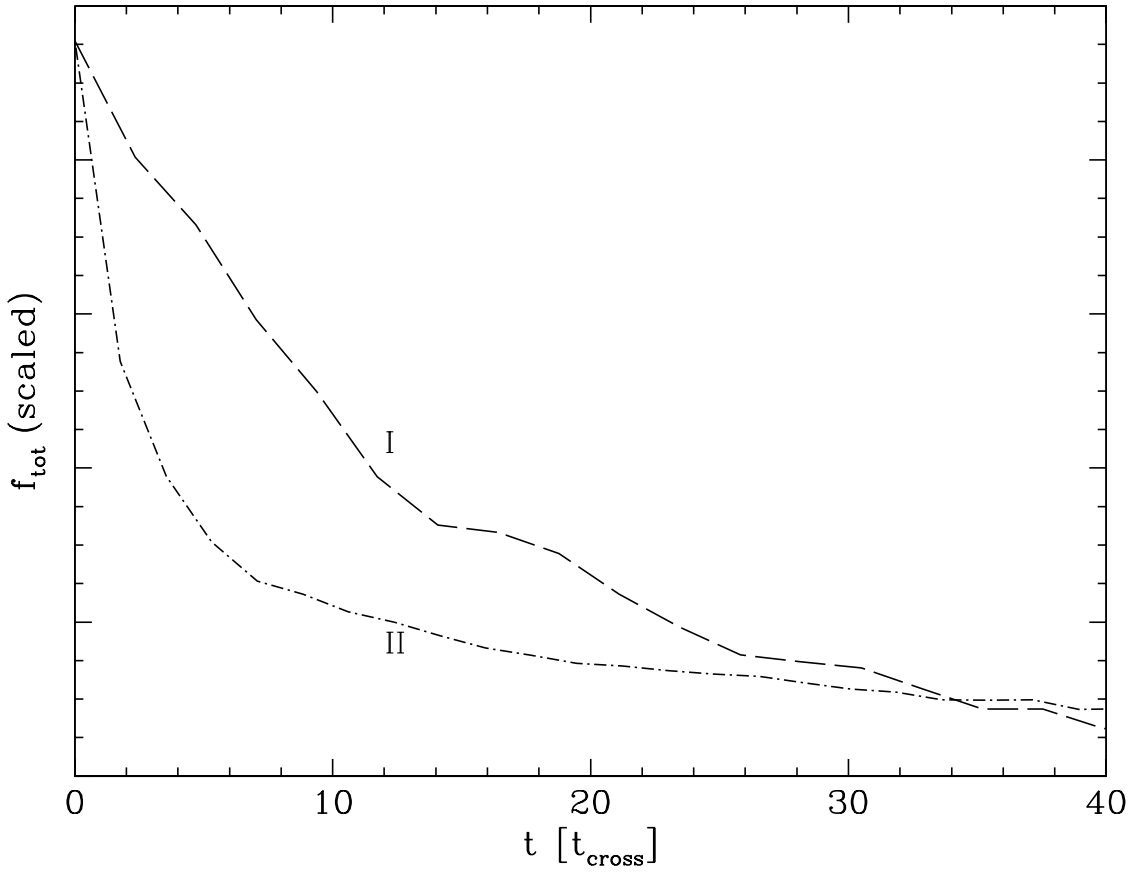

Fig. 1.— Depletion of the binary proportion in two very different clusters. The time-scale is in units of the initial crossing time, whereas the vertical axis is scaled to the minimum and maximum $f_{\rm tot}$. The long-dashed curve (I) is the average of five N-body renditions of a cluster with initially 200 binaries and a Plummer density distribution with $R_{0.5} = 2.5$ pc ($\rho_{\rm c} = 13$ stars/pc^3), and stars with masses in the range 0.1 to 1.1 $M_\odot$ (from Kroupa 1995). The initial crossing time is 18 Myr, the initial $f_{\rm tot} = 1.00$, and the final $f_{\rm tot} = 0.83$. The short-dash-dotted curve (II) is for model A1 in KPM (and this paper; $\rho_{\rm c} = 10^{5.92}$ stars/pc^3), for which the initial $f_{\rm tot} = 0.76$ (reduced from unity because of disruption through crowding, see KPM), the final $f_{\rm tot} = 0.34$, and initial $t_{\rm cross} = 0.059$ Myr. For the virial–equilibrium models discussed in this paper, $f_{\rm tot}(t)$ will lie between the two extreme cases shown here.

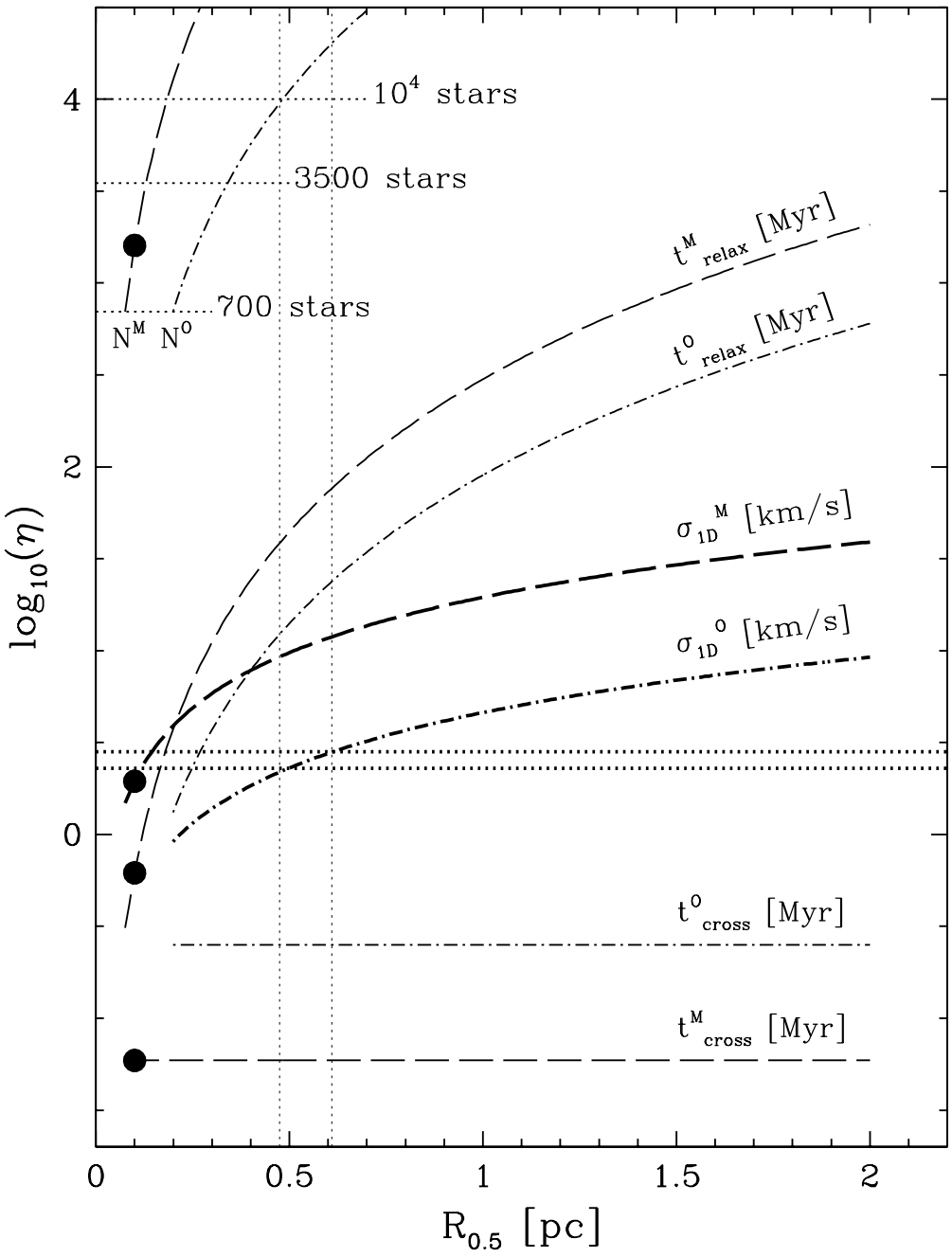

Fig. 2.— Two sets of initial model clusters in virial equilibrium indicated by the super-scripts M (long-dashed curves) and O (short-dash-dotted curves). M refers to models that have the same initial density as models A, and O refers to models with a central density equal to the observed value in the Trapezium Cluster. The number of stars, $\eta = N$, the relaxation time, $\eta = t_{\rm relax}$, and crossing time, $\eta = t_{\rm cross}$, and the one-dimensional velocity dispersion, $\eta = \sigma_{\rm 1D}$, are plotted as $\log_{10}[\eta(R_{0.5})]$ for each model. For example, models A have initially $R_{0.5} = 0.1$ pc with $N = 1600$, $\log_{10}(t_{\rm cross}) = -1.23$ (Myr), $\log_{10}(t_{\rm relax}) = -0.21$ (Myr) and $\log_{10}(\sigma_{\rm 1D}) = 0.29$ (km/s). These are identified by the large black dots. The thin vertical dotted lines delineate the possible set of equilibrium solutions: O-models with $0.48 < R_{0.5} < 0.61$ pc have the same central density as the Trapezium Cluster, and a velocity dispersion consistent within the one-sigma uncertainty range with the observed value, which is shown by the two horizontal dotted lines.

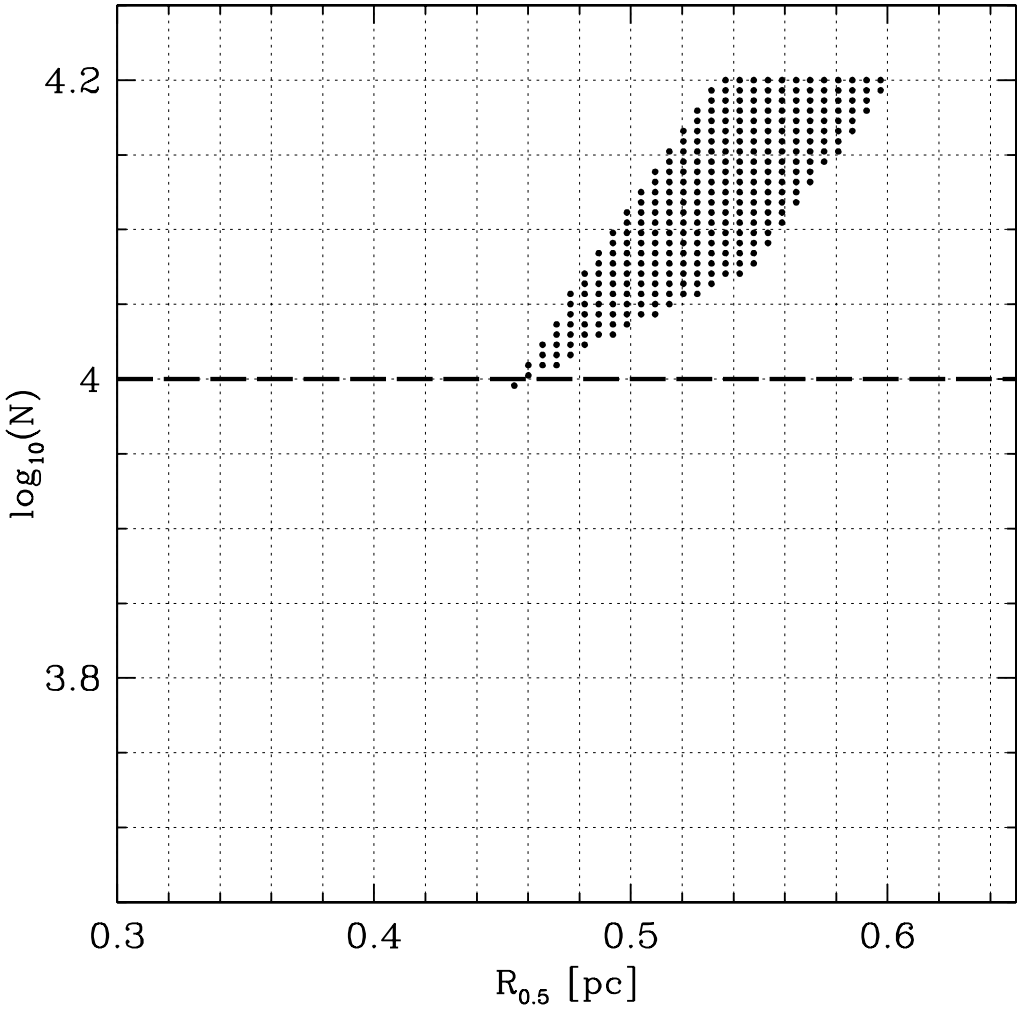

Fig. 3.— The full set of candidate initial cluster models in virial equilibrium. The solution set is obtained by constructing a grid of models with different $R_{0.5}$ and N, and selecting only those that simultaneously satisfy $2.27 \leq \sigma_{1D} \leq 2.81$ km/s, $23.6 \leq n_c \leq 34.4$ stars and $t_{cross} \leq 0.50$ Myr, where n_c is the number of stars in the central volume with radius $R = 0.053$ pc. The boundaries on σ_{1D} are the one-sigma uncertainty range on the observed value. The limits on n_c are $29 \pm \sqrt{29}$. Note that $N \geq 10^4$ must also be excluded because this many stars were certainly not present in the ONC when it was born.

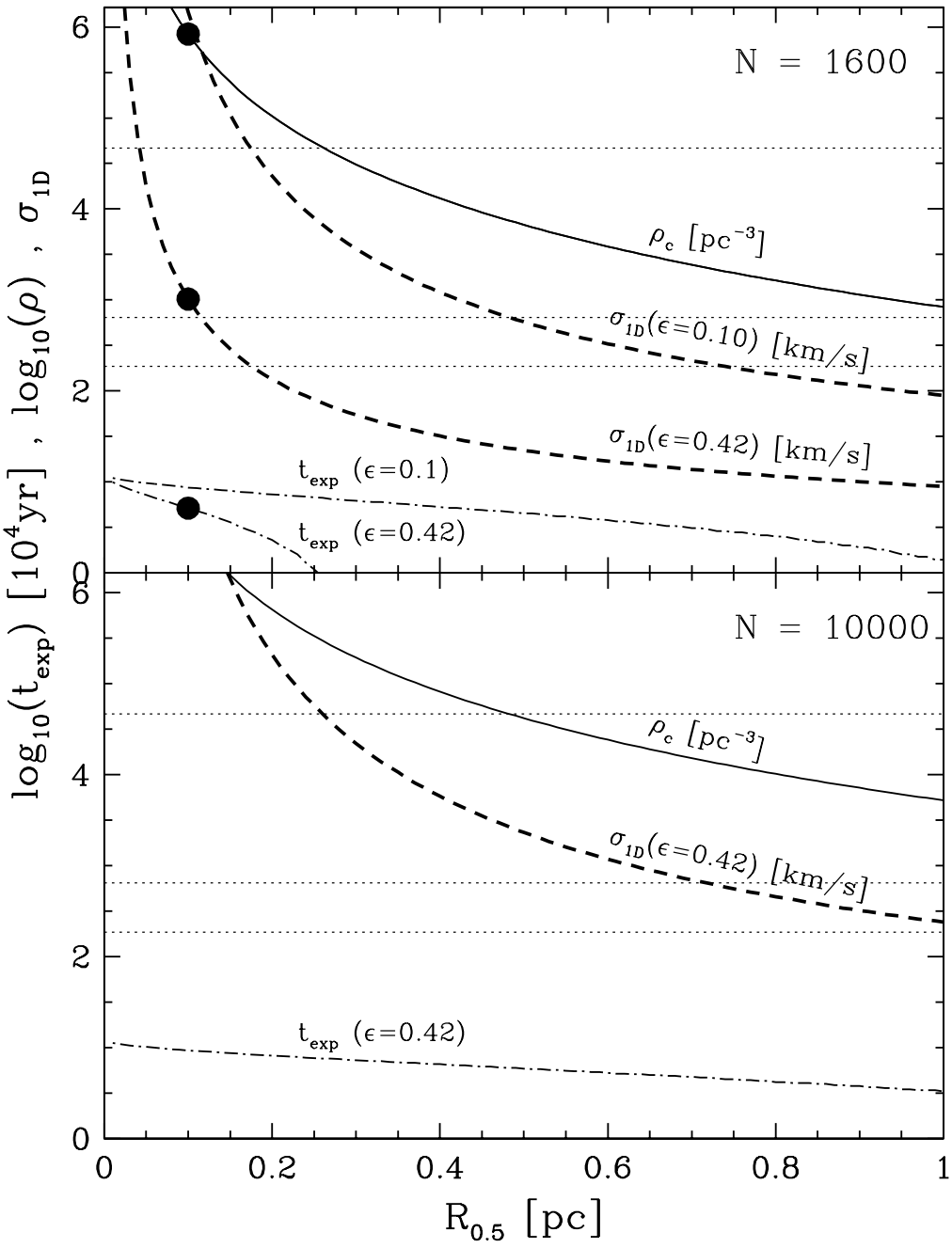

Fig. 4.— Three sets of possible initial model clusters that expand as a result of instantaneous gas loss. The upper panel displays two sets of models for $N = 1600$, and the lower panel shows one set of models for $N = 10^4$. For each model the initial central density, $\log_{10}(\rho_c)$, is plotted as the solid line, the pre-expansion velocity dispersion, $\sigma_{1D}(0)$, is plotted as thick short-dashed curves for star-formation efficiencies $\epsilon = 0.42$ and 0.10, and the time, $\log_{10}(t_{exp})$, when $\sigma_{1D}(t_{exp}) = 1.73$ km/s (the three-sigma lower limit on the observed velocity dispersion) is shown as the dash-dotted line. The lower three-sigma value is used to provide an upper boundary on t_{exp} for each $R_{0.5}$. The one-sigma uncertainty range on the observed velocity dispersion is represented by the two lower horizontal dotted lines, and the upper horizontal dotted line is the observed central density, $\log_{10}(\rho_c^{(obs)})$ in the Trapezium Cluster. For example, for model B2, $\log_{10}(\rho_c) = 5.92$ [stars/pc^3], $\sigma_{1D}(0) = 3.01$ km/s and $\log_{10}(t_{exp}) = 0.72$ [10^4 yr], i.e. $t_{exp} = 5.2 \times 10^4$ yr (large black dots). This is the solution found by KPM.

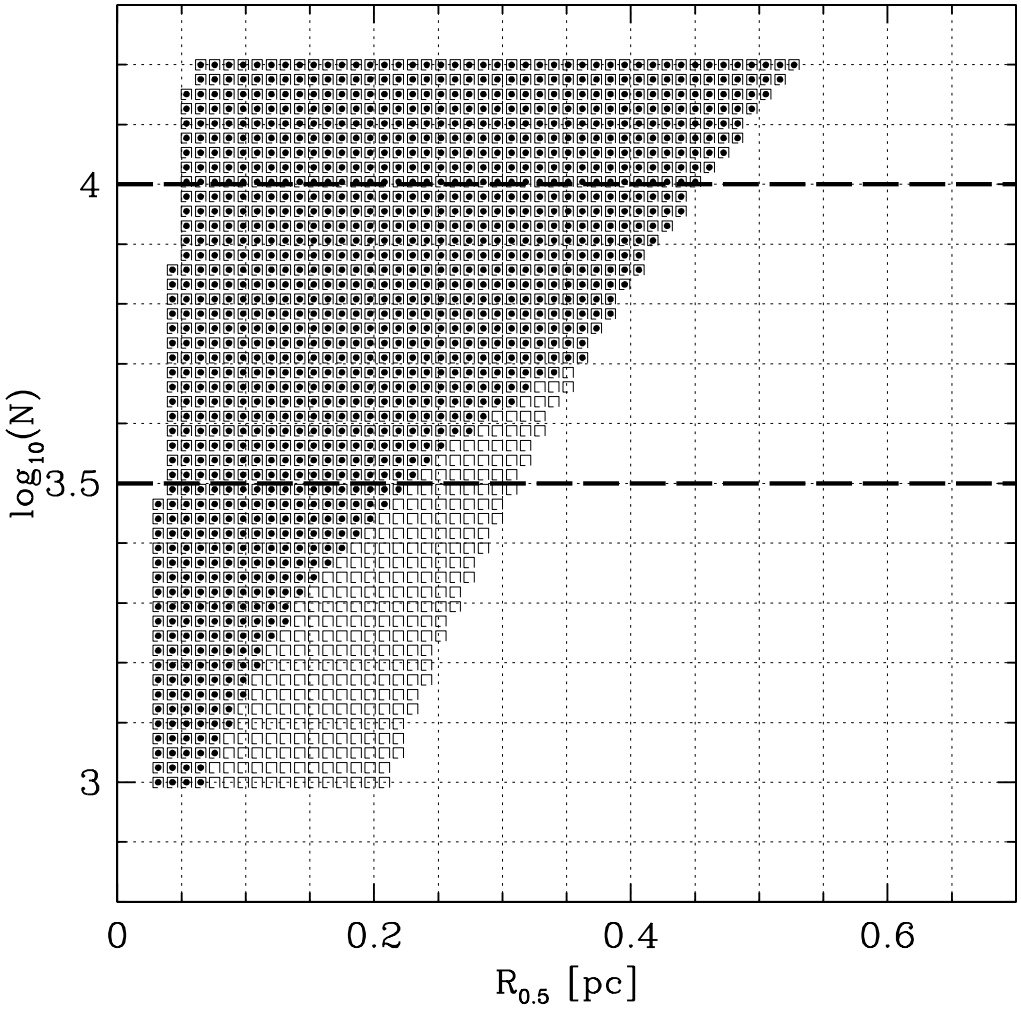

Fig. 5.— The full set of candidate initial models for expanding clusters. The candidate solutions satisfy simultaneously $\sigma_{1D} > 2.81$ km/s, $n_c > 34.4$ stars (see Fig. 3) and $\rho_c \leq 10^{7.69}$ stars/pc^3. Black dots are for a star-formation efficiency $\epsilon = 0.42$, and open squares are for $\epsilon = 0.1$. Note that $\log_{10}(N) < 3.5$ should be excluded because at least 3500 ONC stars have been seen, and $N \geq 10^4$ must be excluded because this many stars were certainly not present in the ONC when it was born.

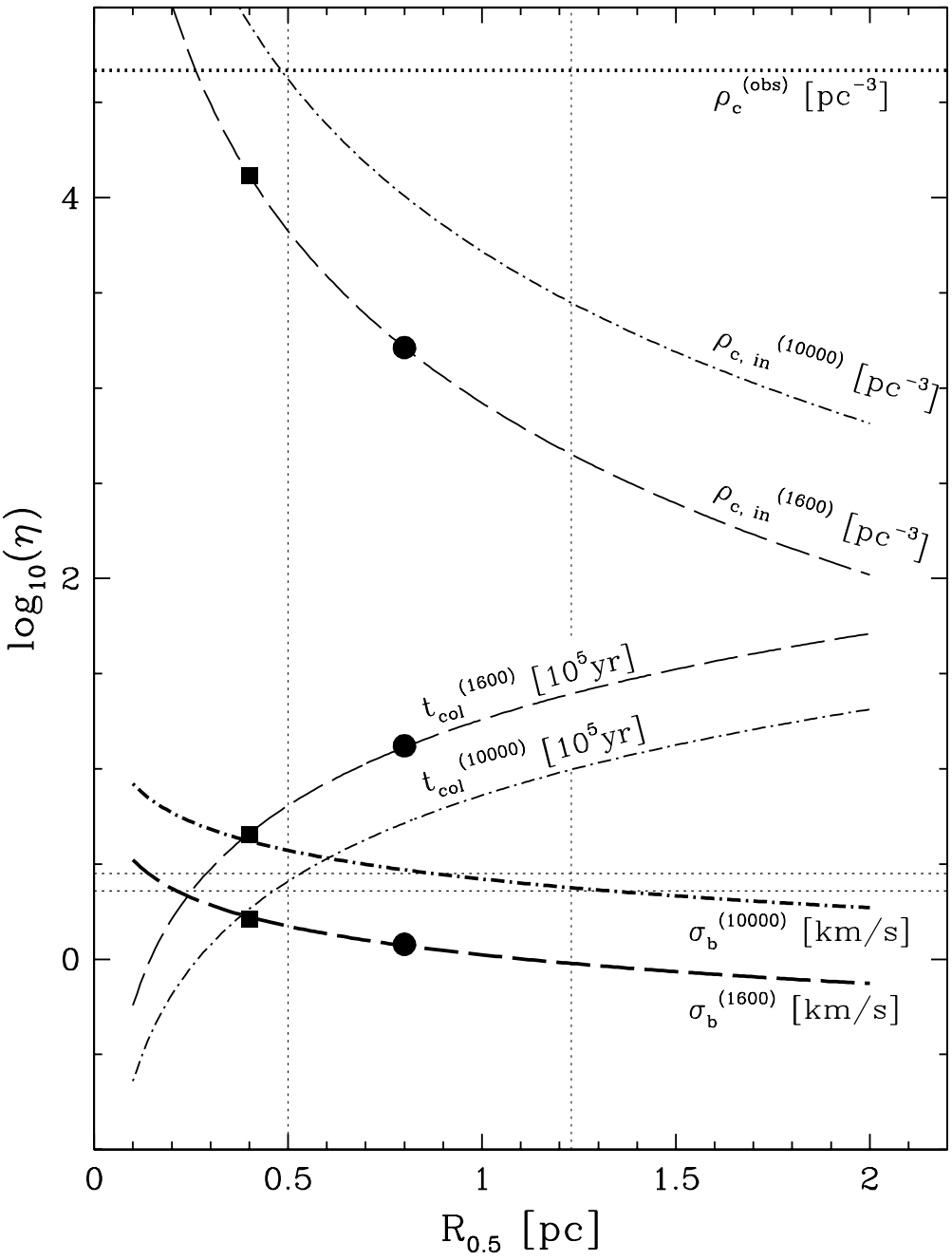

Fig. 6.— Two sets of possible pre-collapse model clusters. Long-dashed curves are for $N = 1600$ and dash-dotted curves are for $N = 10^4$. For each, $\log_{10}(\eta)$ is plotted in dependence of $R_{0.5}$, with $\eta = \rho_{\rm c,in}, t_{\rm col}, \sigma_{\rm b}$. For example, model C1 has $\rho_{\rm c,in} = 1.3 \times 10^4$ stars/pc^3, and from fig. 10 in KPM, $t_{\rm col} = 0.45$ Myr and $\sigma_{\rm b} = 1.62$ km/s (black squares), and model C2 has $\rho_{\rm c,in} = 1.6 \times 10^3$ stars/pc^3, and from fig. 10 in KPM $t_{\rm col} = 1.32$ Myr and $\sigma_{\rm b} = 1.20$ km/s (black circles). The upper horizontal dotted line is the presently observed central density in the Trapezium Cluster, and the two lower horizontal lines show the one-sigma range of the observed velocity dispersion. The two vertical dotted lines delineate the candidate solution set for $N = 10^4$, the left boundary being determined by $\rho_{\rm c,in} \leq \rho_{\rm c}^{\rm (obs)}$ and the right boundary by $\sigma_{\rm b} \geq \sigma^{\rm (obs)}$. Models with $0.5 < R_{0.5} < 1.23$ pc are thus expected to satisfy the observational constraints as they collapse with collapse times $t_{\rm col} < 10^6$ yr. There is no set of solutions for models with $N = 1600$, because when $\sigma_{\rm b} \geq \sigma^{\rm (obs)}$, $\rho_{\rm c,in}$ is larger than the observed density.

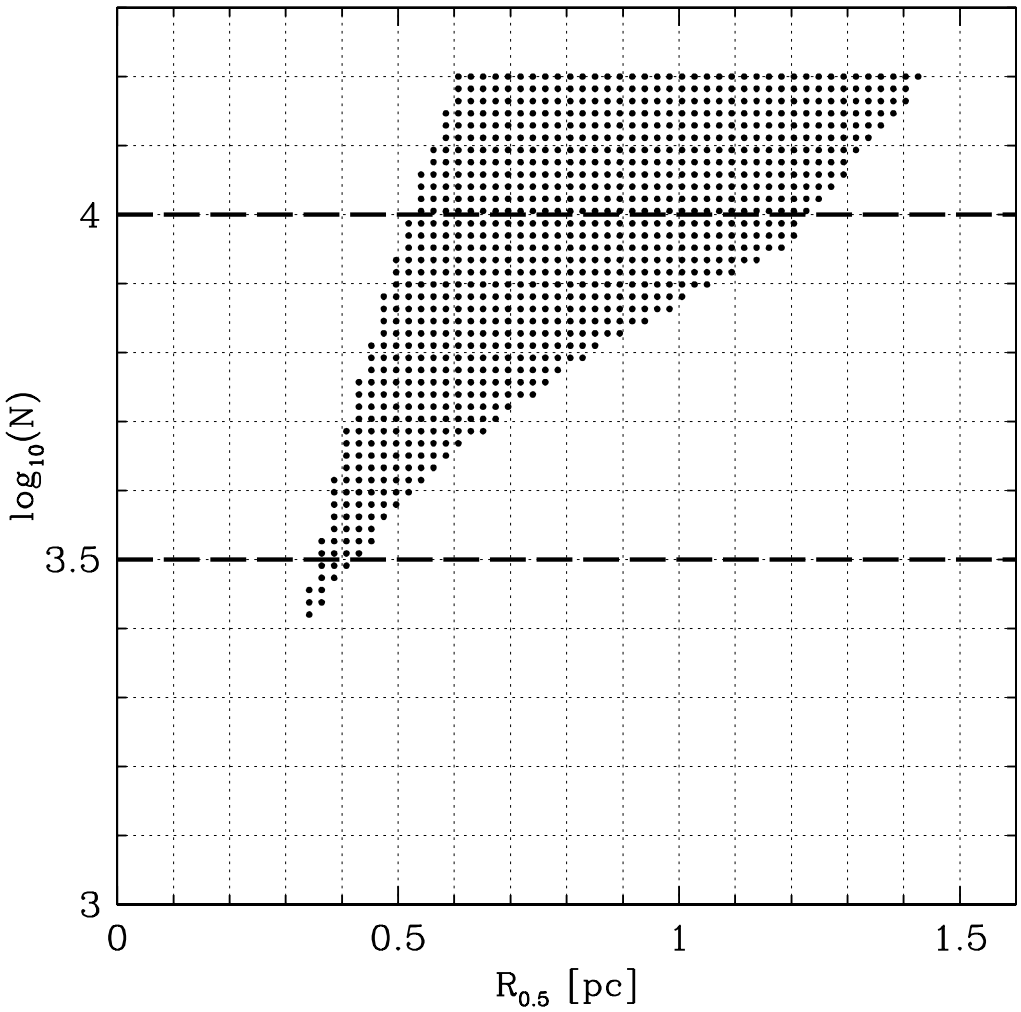

Fig. 7.— The full set of candidate initial models of collapsing clusters. The candidate solutions satisfy simultaneously $\sigma_{\rm b} > 2.27$ km/s, $n_{\rm c} < 23.6$ stars (see Fig. 3) and $t_{\rm col} < 1$ Myr. Note that $\log_{10}(N) < 3.5$ should be excluded because at least 3500 ONC stars have been seen, and $N \geq 10^4$ must be excluded because this many stars were certainly not present in the ONC when it was born.